Combinatorial invariants and covariants as tools for conical intersections

Itai Ryb and Roi Baer[a)]
Department of Physical Chemistry and the Lise Meitner Minerva-Center for Quantum Chemistry, The Hebrew University of Jerusalem, Jerusalem 91904, Israel

(Received 25 June 2004; accepted 31 August 2004)

The combinatorial invariant and covariant are introduced as practical tools for analysis of conical intersections in molecules. The combinatorial invariant is a quantity depending on adiabatic electronic states taken at discrete nuclear configuration points. It is invariant to the phase choice (gauge) of these states. In the limit that the points trace a loop in nuclear configuration space, the value of the invariant approaches the corresponding Berry phase factor. The Berry phase indicates the presence of an odd or even number of conical intersections on surfaces bounded by these loops. Based on the combinatorial invariant, we develop a computationally simple and efficient method for locating conical intersections. The method is robust due to its use of gauge invariant nature. It does not rely on the landscape of intersecting potential energy surfaces nor does it require the computation of nonadiabatic couplings. We generalize the concept to open paths and combinatorial covariants for higher dimensions obtaining a technique for the construction of the gauge-covariant adiabatic-diabatic transformation matrix. This too does not make use of nonadiabatic couplings. The importance of using gauge-covariant expressions is underlined throughout. These techniques can be readily implemented by standard quantum chemistry codes. © *2004 American Institute of Physics.* [DOI: 10.1063/1.1808695]

I. INTRODUCTION

Conical intersections[1] (CIs) of adiabatic potential energy surfaces (PES) in molecules offer an efficient and fast mechanism to convert electronic excitation energy into nuclear vibrational or translational motion. These nonadiabatic effects are crucial steps in many photochemical processes[2–9] of importance in biology and organic chemistry. However, CIs may even affect adiabatic processes because of the nonlocal effects they have on the nuclear dynamics.[10–12]

The CIs are surfaces of dimension D—2 in the D-dimensional nuclear configuration space [when the electronic Hamiltonian is complex Hermitian, as in certain cases when spin-orbit coupling is taken into account, the dimensions can be D—2, 3, 5 (Refs. 13 and 14)]. In three-dimensional (3D) projections of D-dimensional space, CIs form one-dimensional strings, which are called seams. On two-dimensional projections CIs appear as (zero-dimensional) points. For molecular dynamics simulations, it is of critical importance to characterize and pinpoint the manifolds of nuclear configurations at which CIs exist.[15] Typically the search for CI points is performed on two-dimensional projections of the nuclear configuration space. Several methods have been devised for this purpose. One class of approaches exploits the unique energy landscape near a CI,[16–18] based on analytical gradients or marching along ridges.[19] Another class of approaches is based on the electronic wave function properties. These exploit the change of sign in the adiabatic electronic wave function when transported on a loop in nuclear configuration space encircling conical intersections.[20] One successful approach to effectively transport the wave function along the loop uses path-ordered exponentials of nonadiabatic coupling terms (NACs), calculated with analytical gradient techniques.[21,22] The benefit of using the wave function method is its being indifferent to the complicated topology of the intersecting PESs. However, a drawback is the use of analytical gradients which make the calculation numerically expensive. A further complication is the need to define the phase (sign in the case of real wave functions) of the electronic wave functions in a consistent (smooth) manner.

An alternative method for wave function transport is to propagate an electronic eigenfunction around the loop using slow (adiabatic) time-dependent evolution. In this case the evolved wave function stays as an eigenfunction but its phase changes with time. Upon completing the loop and returning to the initial point, a comparison of the phases can be made. The accumulated phase during evolution minus the time integral of the adiabatic energy is called the Berry phase β. Berry showed that β dependsonthe loop itself and not on the details of how it was transported. In the case of real electronic Hamiltonians, β can only be an integer multiple of π. In this case, it follows from Berry's theory that almost any 2D surface (embedded in the D-dimensional nuclear configuration space) bounded by the loop will contain an even number of CI points (including zero) if $\beta = 0 \bmod 2\pi$ and an odd number if $\beta = \pi \bmod 2\pi$. Using this adiabatic process for calculating the Berry phase thereby determining the presence of CIs has several advantages: absence of derivatives with respect to the nuclei and independence of arbitrary phase choices. It is nevertheless computationally cumbersome since the adiabatic evolution may be numerically expensive.

a)Author to whom correspondence should be addressed. Electronic mail: roi.baer@huji.ac.il

This paper discusses a wave function method for locating the CI. We use a combinatorial (discrete) gauge invariant, i.e., a discrete quantity indifferent to the phase choice of the adiabatic states. The combinatorial invariant was first developed for analyzing the macroscopic polarization in crystals by King-Smith and Vanderbilt[23] and Resta,[24,25] based on the concept of the Pancharatnam phase.[26] In a certain limit this discrete invariant is equal to the phase change along a loop. The combinatorial invariant enjoys two benefits over the existing wave function methods: (1) there is no need to compute nonadiabatic couplings (and therefore no need for analytical derivatives) and (2) there are no phase indeterminacy problems. The only numerical machinery is the overlap between adiabatic states corresponding to two different nuclear configurations.

Once the CIs are located special methods to perform the dynamics are needed. One problem is that the NACs become singular at CIs prohibiting efficient numerical calculations. A common cure for this problem is diabatization.[27–30] In the original diabatization method[27] an adiabatic to diabatic transformation (ADT) is constructed for N states along a path. The ADT matrix is gauge covariant: it transforms under a gauge change according to the phase changes in the first and last point of the path.[31] The actual calculation of the ADT is complicated by the need to compute NACs for many points along the given path. The procedure to ensure covariance is complicated because the methods used do not assure it automatically. We present a method for constructing the ADT matrix along the given path. We extend the concept of the combinatorial invariant to a combinatorial covariant *matrix product* which in a certain limit yields the ADT. For any finite number of points it is of course only an approximation to the ADT. But even then, it is by construction gauge covariant thus having the exact gauge transformation properties of the exact ADT. This is an important advantage. In this method there are no NACs to be calculated and phase/sign smoothness problems do not arise.

The combinatorial invariant is described in Sec. II. Using it, we develop in Sec. III the algorithms for pinpointing the CI, demonstrating their performance on a simple model system. Finally, in Sec. IV we derive the combinatorial matrix product and show its utility as a method for computing the ADT. Section V summarizes and discusses the results.

II. THE COMBINATORIAL INVARIANT

Consider a set of nuclear configurations (points) $\mathbf{R}^\alpha$, $\alpha=1,\ldots,M$ and associated eigenfunctions of the electronic Hamiltonian at $\mathbf{R}^\alpha$, $\hat{H}_e[\alpha]$:

$$\hat{H}_e[\alpha]|\alpha;j\rangle = V_j[\alpha]|\alpha;j\rangle, \quad j=1,2,.... \tag{2.1}$$

We follow henceforth the standard nomenclature and call $|\alpha;j\rangle$ the jth adiabatic electronic wave function at $\mathbf{R}^\alpha$. The combinatorial invariant is defined[24] as

$$I_j^{(M)} = \langle 1;j|2;j\rangle\langle 2;j|3;j\rangle\cdots(M;j|1;j\rangle = \langle 1;j|\hat{P}_{2;j}\hat{P}_{3;j}\cdots\hat{P}_{M;j}|1;j\rangle. \tag{2.2}$$

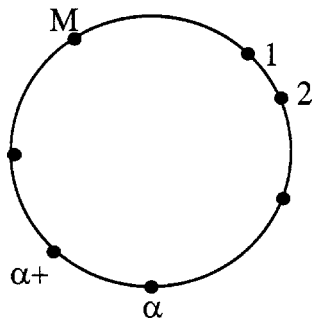

FIG. 1. A set of points in nuclear configuration space placed along a loop.

Under this notation $\langle\alpha;j|\alpha';j\rangle$ is an overlap integral of two electronic wave functions, performed over all electronic degrees of freedom. The invariant can be viewed as a product of overlaps or as the expectation value of a product of projection operators $\hat{P}_{\alpha;j}\equiv|\alpha;j\rangle\langle\alpha;j|$ on the jth adiabatic state at point α. It is glaringly obvious that $I_j^{(M)}$ is invariant to the choice of the phase of the adiabatic wave functions, i.e., to the gauge transformation induced by

$$|\alpha;j\rangle \to \overline{|\alpha;j\rangle} = e^{i\theta_{\alpha,j}}|\alpha;j\rangle. \tag{2.3}$$

Consider now a closed path (or simply a loop) Λ in nuclear configuration space, not passing through a conical intersection, and take the points $\mathbf{R}^\alpha$ to lie on this loop (Fig. 1). One can increase the number of points on Λ so they cover the loop in the following limit:

$$\delta R \equiv \max_\alpha|\delta\mathbf{R}^\alpha| \to 0 \quad \text{and} \quad M\to\infty, \tag{2.4}$$

where $\delta\mathbf{R}^\alpha=\mathbf{R}^{\alpha+1}-\mathbf{R}^\alpha$. We now show that in this limit

$$\lim_{M\to\infty} I_j^{(M)} = e^{i\beta_j(\Lambda)}, \tag{2.5}$$

where β_j is the Berry phase for the jth adiabatic state along the loop. The Berry phase is defined using a smooth, single-valued, and differentiable set of adiabatic states along the loop $\psi_j(\mathbf{R})$, by evaluating the following expression:[32]

$$\beta_j(\Lambda) = -i\oint_\Lambda \tau_{jj}^\mu(\mathbf{R})dR_\mu, \tag{2.6}$$

where $\tau_{jj}^\mu=\langle\psi_j(\mathbf{R})|\partial^\mu\psi_j(\mathbf{R})\rangle$ is an imaginary function (and $\partial^\mu\equiv\partial/\partial R_\mu$), μ indexes the nuclear degrees of freedom, and the Einstein summation convention is used for repeated μ indices. One easily sees that for small δR,

$$\begin{aligned} e^{i\beta_j(\Lambda)} &= \exp\left[\oint_\Lambda \tau_{jj}^\mu(\mathbf{R})dR_\mu\right] \\ &= [1+\tau_{jj}^\mu(\mathbf{R}^1)\,\delta R_\mu^1][1+\tau_{jj}^\mu(\mathbf{R}^2)\,\delta R_\mu^2]\cdots \\ &\quad\times[1+\tau_{jj}^\mu(\mathbf{R}^M)\,\delta R_\mu^M]+O(\delta R^2). \end{aligned} \tag{2.7}$$

We now use Taylor's expansion,

$$\psi_j(\mathbf{R}+\delta\mathbf{R}) = \psi_j(\mathbf{R}) + \partial^\mu\psi_j(\mathbf{R})\,\delta R_\mu + O(\delta\mathbf{R}^2), \tag{2.8}$$

to compute each term in the product of Eq. (2.7) as an overlap:

$$\langle\psi_j(\mathbf{R})|\psi_j(\mathbf{R}+\delta\mathbf{R})\rangle = 1+\tau_{jj}^\mu(\mathbf{R})\,\delta R_\mu + O(\delta\mathbf{R}^2). \tag{2.9}$$

Combining with Eq. (2.7) in the limit $\delta\mathbf{R}\to 0$, Eq. (2.5) is thus proved for the special case that $|j;\alpha\rangle = |\psi_j(\mathbf{R}_\alpha)\rangle$. However, this must now also hold for any choice of $|j;\alpha\rangle$ since it differs from $|\psi_j(\mathbf{R}_\alpha)\rangle$ by at most a phase factor and $I_j^{(M)}$ is invariant to *any* phase choice. We further note that one can also use in the combinatorial invariant real adiabatic states for estimating the Berry phase, while a complex basis must be used for evaluating Eq. (2.6) (actually, for real adiabatic states $\tau_{jj}\equiv 0$). When extending the result of Eq. (2.9) to second order, one can derive

$$\langle \alpha;j|\alpha+1;j\rangle = \sqrt{1-\sum_{k\neq j}|\tau_{jk}^{\mu}(\mathbf{R}^{\alpha})\,\delta R_{\mu}^{\alpha}|^2}\,\exp[\,\tau_{jj}^{\mu}(\mathbf{R}^{\alpha})\,\delta R_{\mu}^{\alpha}] + O(\delta R^3). \tag{2.10}$$

This shows that the loss of modulus is associated with coupling to other adiabatic states through the off-diagonal elements of the NAC matrix.

III. LOCATING CONICAL INTERSECTIONS

The process of locating CIs consists of recursively generating closed loops that zoom in on a certain CI. Thus, two procedures are necessary: a verification procedure which allows us to determine if a CI is in a certain loop and the location procedure breaking up a verified loop into a number of smaller loops, each a new candidate for verification.

Let us first discuss the process of verification. Suppose Γ is a closed path, a loop, and we want to determine if a CI is encircled by it. We assume that it is known that a single CI exists in the region. If an even number of CIs coexist one in the vicinity of the other, our algorithm may fail and a refinement of the loop is needed. In order to verify, we distribute M points along the path and compute $I^{(M)}$. Usually some points already exist on the path from previous iterations of the verification-location procedure. How can we determine if the phase of $I^{(M)}$ accurately represents the Berry phase $\beta(\Gamma)$ [see Eq. (2.5)]? Since the norm $|I^{(M)}|$ should converge to 1 when $M\to\infty$, the positive number $\varepsilon^{(M)}=1-|I^{(M)}|$ is used to determine the accuracy of $I^{(M)}$ as an approximation to $e^{i\beta}$. We set an accuracy criterion δ and continuously add points on the loop, increasing M, until $\varepsilon^{(M)}<\delta$. One way to add points is the naïve approach. At each iteration a point is added in between every two points of the previous iteration, thus each overlap $\langle\alpha;j|\alpha+1,j\rangle$ of the previous iteration is replaced by $\langle\alpha;j|\alpha',j\rangle\langle\alpha';j|\alpha+1,j\rangle$ in the new iteration. Such a process doubles the number of points at each iteration.

The problem with the naïve approach is that an excessive number of points might be required for convergence. We present a better approach, we call the *adaptive method*, that acknowledges the fact that at each new point a numerically expensive step is required, namely, the calculation of the adiabatic state. Supposing we already have M points distributed on the path, it is important to determine where the next point $\mathbf{R}^{M+1}$ is likely to be most effective at reducing $\varepsilon^{(M)}$. We set to do this by searching for the "weakest link" α^* according to the following procedure:

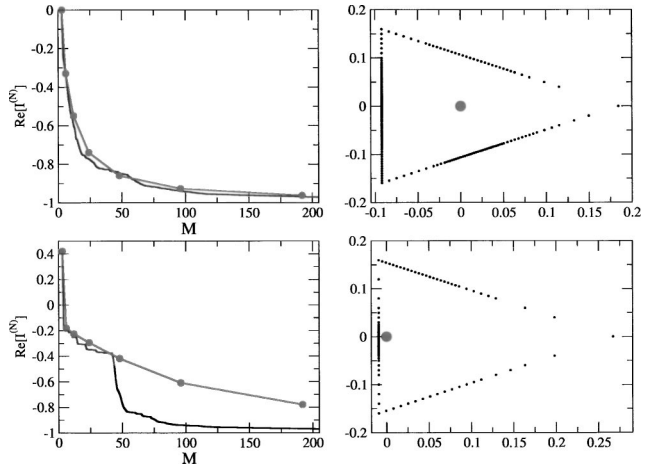

FIG. 2. The verification algorithm for a triangular loop in two cases. Top: isotropic CI (large dot) in the middle of the triangular loop; Bottom anisotropic CI close to the edge of the loop. On the left—the convergence of the invariant $I^{(M)}$ to -1 as a function of number of sampling points: the naïve (dotted line) and the adaptive (continuous line) algorithms. The location of the points generated by the adaptive algorithm is shown on right panels. The linear density of points is indicative of the strength of the NAC field.

$$d_{\alpha^*}=\min_{\alpha} d_\alpha;\; d_\alpha=|\langle\alpha|\alpha+1\rangle|. \tag{3.1}$$

Once the link α^* is determined, the next point $\mathbf{R}^{M+1}$ is taken as a point on the path between $\mathbf{R}^{\alpha^*}$ and $\mathbf{R}^{\alpha^*+1}$. The process is repeated until the convergence criterion $\varepsilon^{(M)}<\delta$ is met.

In order to demonstrate the performance of the verification algorithm, we have considered a Longuet-Higgins type of Hamiltonian,

$$\hat{H}(R,\phi)=-\tfrac{1}{2}\boldsymbol{\nabla}^2+r^2+2R\cos[2\theta+f_\zeta(\phi)], \tag{3.2}$$

where r,θ are the "electronic" coordinates while R,ϕ are "nuclear" parameters. This Hamiltonian exhibits a CI at the parameter origin ($R=0$) in the 1st and 2nd excited states, due to the degeneracy of the azimuthal angular momentum $|m|=1$. The function $f_\zeta(\phi)=(1-\zeta)\phi+2\pi\zeta\sin^2(\phi/4)$ is used to insert anisotropy (the existence of CI anisotropy in actual molecules has been demonstrated[33]) into the Longuet-Higgins model ($\zeta\neq 0$). A computer implementation represents the wave functions on a two-dimensional Cartesian Fourier grid, using fast Fourier transform methods for affecting the kinetic energy. The angular potential is written in Cartesian coordinates as

$$2R\cos(2\theta-f_\zeta)=\frac{2}{R}[(x^2-y^2)\cos f_\zeta+2xy\sin f_\zeta]. \tag{3.3}$$

A 2D grid of 32×32 points was required for converging the solution to sufficient accuracy. The adiabatic states were generated by diagonalizing the 1024×1024 Hamiltonian matrix.

In Fig. 2 we show the performance of the algorithm for two typical cases. The loop is a triangular path enclosing the CI. The two top panels are for the case where the CI is isotropic ($\zeta=0$) and in the center of the triangular loop. On the left a graph is shown that depicts $I^{(M)}$ as a function of M. The points generated by the adaptive algorithm are shown on

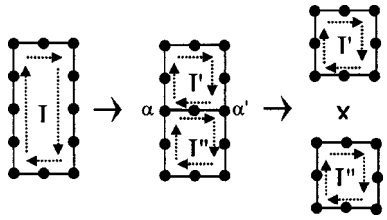

FIG. 3. The spawning of the invariant corresponding to a rectangular loop I into two invariants $I' \times I''$ corresponding to smaller loops.

the right top panel. The algorithm automatically places a higher concentration of points on the loop where the NAC field is higher. At the lower two panels we show the case where the CI is both anisotropic ($\zeta = 1$) and very close to one of the segments of the triangle. In this case the adaptive algorithm is considerably more efficient than the naïve algorithm and near convergence is achieved with about 200 points. Looking at the right lower panel, we notice the anisotropy and inhomogeneities in the placement of the points. Once again, the segments with higher concentration of points correspond to higher NAC fields. These results show that the adaptive method not only is more efficient in tough cases, but also maps out the field of the NACs. This will be more evident in the location procedure we discuss next.

Location is the process of breaking up a verified loop, i.e., a loop for which the phase $Ph(I)$ is π into several (two or more) new loops. Here, we tested two approaches having comparable efficiency. The first is a bisection method, where the paths are all rectangles. At each stage the current rectangle invariant I is bisected into two rectangle invariants I' and I'' of equal area by bisecting the long edges using a segment $\alpha\alpha'$ as shown in Fig. 3. The bisecting segment is padded with sampling points $\tilde{\alpha}_1, \ldots, \tilde{\alpha}_m$, according to the adaptive algorithm until its open-path product $\tilde{I}_{\alpha\alpha'}$ is sufficiently converged. It is straightforward to see that

$$I = I' I'' / |\tilde{I}|^2. \tag{3.4}$$

Thus the total phase is conserved:

$$Ph(I) = Ph(I') + Ph(I''). \tag{3.5}$$

Only two possibilities arise: either $Ph(I') = \pi$ or $Ph(I'') = \pi$. In the former case the process is iterated for loop I' while in the latter, for loop I''. The behavior of this bisection location algorithm is examined in Fig. 4, panel (a) for an isotropic CI and panel (c) for an anisotropic CI. In both cases, the CI is placed close to the middle of the initial rectangle. The effect of the adaptive algorithm is easily observed as points are distributed on the segments in varying concentration. The densely sampled regions are those closer to the CI or those that are shined upon by the anisotropic CI.

A second method of location is based on triangular paths. It is somewhat less efficient but has the added merit in that it reveals the structure of the vector field τ_{jj} using the various segments created. We start with a verified triangular loop (i.e., a loop known to have a CI) and at each stage we decompose it using a new inner triangle, whose edges are bisectors of the original triangle (Fig. 5). This process produces four smaller similar triangles. The middle triangle (IV)

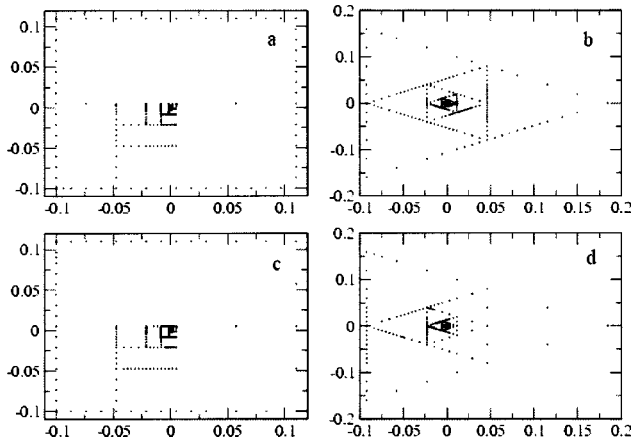

FIG. 4. The sampling points used by the adaptive verification-location algorithm for rectangular (a,c) and triangular (b,d) methods, for two cases: isotopic (a,b) and anisotropic (c,d) CI. The CI is always at the origin of the X-Y coordinate system.

is verified first, and if the CI is not encircled by it, there are already enough points on the edges of the other three triangles to determine which of them does. The method is demonstrated in Fig. 4 panel (b) (isotropic CI) and (d) (anisotropic CI). The process efficiently zooms in on the CI, with the added benefit that the generated points reflect the strength of the NAC field. This is because the adaptive algorithm places points at places where the NAC field is high.

Both rectangular and triangular location algorithms have comparable efficiency, with somewhat better performance for the former. The fact that the triangulation also charts out the NAC field is a big bonus since it allows us to determine where nonadiabtic effects may be important.

IV. THE COMBINATORIAL COVARIANT

In order to perform a nonadiabatic dynamical calculation in the presence of CIs, describing N electronic eigenfunctions (adiabatic states), it is necessary to evolve the nuclear wave packets $\chi_j(\mathbf{R},t)$, $j = 1,\ldots,N$ using the following set of Schrödinger-like equations, derived from the Born-Oppenheimer picture:[34,35]

$$i\dot{\chi}(\mathbf{R}) = \frac{1}{2M_\mu}(\partial^\mu - \tau^\mu)^2 \chi + U\chi. \tag{4.1}$$

Here M_μ is the nuclear mass associated to the μth nuclear degree of freedom, χ is a column vector of the N

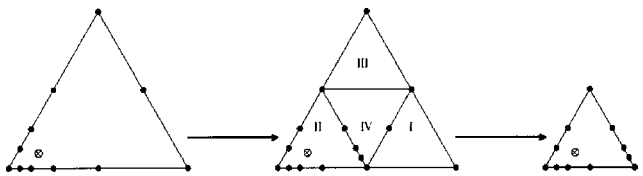

FIG. 5. The triangular location method. A verified triangular loop (CI is the open circle) is decomposed into four subloops by inner bisecting segments. The inner triangle (IV) is verified first, by using the adaptive algorithm to add points along the inner perimeter. Using these points one of the inner triangles is found to contain the CI.

nuclear wave packets, U is a $N\times N$ diagonal matrix of the adiabatic potential energy surfaces, and τ is the $N\times N$ matrix of nonadiabatic couplings (NACs):

$$\tau^{\mu}_{jk}(\mathbf{R})=\langle \mathbf{R};j|\partial^{\mu}\mathbf{R};k\rangle. \tag{4.2}$$

These NACs are typically singular at CIs, causing numerical instabilities when the nuclear wave packet overlaps the CI. In this case it is beneficial to *diabatize*, i.e., affect a unitary transformation on Eq. (4.1) that removes the presence of NACs at the expense of making the potential matrix nondiagonal, leading to

$$i\dot{\tilde{\chi}}(\mathbf{R})=\frac{1}{2M_{\mu}}(\partial^{\mu})^2\tilde{\chi}+W\tilde{\chi}. \tag{4.3}$$

The unitary transformation matrix that achieves the diabatization is the $N\times N$ matrix $A(\mathbf{R})$ through which

$$\begin{aligned}&\tilde{\chi}(\mathbf{R},t)=A(\mathbf{R})\chi(\mathbf{R},t),\\ &W(\mathbf{R})=A(\mathbf{R})U(\mathbf{R})A(\mathbf{R})^{\dagger}.\end{aligned} \tag{4.4}$$

The conditions for which the procedure gives well-defined diabatic potentials W has been studied thoroughly elsewhere.[36] In general, diabatization is an approximation. In a certain region of nuclear configuration space it is possible to choose enough adiabatic states N such that the approximation is well controlled. A criterion for this case has been developed using ADT matrices *along loops* (we define this matrix bellow[36]): ideally these must be diagonal. In the real electronic Hamiltonian case the diagonal elements are either 1 or -1, a condition known as the quantization condition for diabatization.[36] Thus the degree of diagonality for all loops in the region of diabatization is indicative of the quality of the diabatization procedure.

The matrix at a point $A(\mathbf{R}^f)$ is computed along a given path[27] Γ in nuclear configuration space connecting a reference point $\mathbf{R}^1$ to $\mathbf{R}^f$. This is done using the expression

$$A(\mathbf{R}^f;\Gamma)=B(\Gamma)A(\mathbf{R}^1), \tag{4.5}$$

where[37]

$$B(\Gamma)=\hat{P}\exp\left[-\int_{\Gamma}\tau^{\mu}\cdot dR_{\mu}\right] \tag{4.6}$$

is a path-ordered exponential of the matrix $\tau^{\mu}dR_{\mu}$. In what follows, we will denote the B matrix as *the* ADT, the multiplication by $A(\mathbf{R}^i)$ is implied.

We now generalize the combinatorial invariant concept to a non-Abelian matrix product. We show in particular that the ADT can be calculated without NACs by a limit of a combinatorial product of matrices:

$$J^{(M)}=\langle M|M-1\rangle\cdots\langle 3|2\rangle\langle 2|1\rangle. \tag{4.7}$$

Here, we select discrete points $\mathbf{R}^{\alpha}$, $\alpha=1,...,M$ (with $\mathbf{R}^M=\mathbf{R}^f$) spread over the path Γ. We continue to use the notation of Sec. II, where $|\alpha;j\rangle$ is the jth adiabatic state at $\mathbf{R}^{\alpha}$. The symbol $\langle\alpha|\alpha+1\rangle$ now denotes an $N\times N$ matrix whose elements are given by

$$\langle\alpha+1|\alpha\rangle_{jk}=\langle\alpha+1;j|\alpha;k\rangle,\quad j,k=1,...,N. \tag{4.8}$$

Let us now take the limit $M\to\infty$ in Eq. (4.7) such that Eq. (2.4) is obeyed. In this limit we show below that

$$\lim_{M\to\infty}J^{(M)}=B(\Gamma)=\hat{P}\exp\left[-\int_{\Gamma}\tau^{\mu}\cdot dR_{\mu}\right]. \tag{4.9}$$

To prove Eq. (4.9), consider an infinitesimal path segment dR connecting $\mathbf{R}^{\alpha}$ and $\mathbf{R}^{\alpha+1}=\mathbf{R}^{\alpha}+\delta\mathbf{R}^{\alpha}+O[(\delta R)^2]$. Using the Taylor expansions Eq. (2.8) and Eq. (4.2), we have

$$\langle\alpha+1;j|\alpha;k\rangle=1-\tau^{\mu}_{jk}(\mathbf{R}^{\alpha})\,\delta R_{\mu}+O(\delta\mathbf{R}^2). \tag{4.10}$$

This holds for all $1\leqslant j,k\leqslant n$ and thus

$$\langle\alpha+1|\alpha\rangle=\exp[-\tau^{\mu}\delta R^{\alpha}_{\mu}]+O[(\delta\mathbf{R})^2]. \tag{4.11}$$

The path-ordered exponential in Eq. (4.9) is defined as the infinite path-ordered matrix product of the infinitesimal exponential matrices appearing on the right of Eq. (4.11). Thus, taking a product of M matrices gives $J^{(M)}$ and in the limit of infinitely many points [in the sense of Eq. (2.4)] will converge to Eq. (4.9).

Using this result for the purpose of diabatization is an efficient way of calculating the adiabatic-diabatic matrix, since it does not require computation of nonadiabatic coupling matrices. An important property of the combinatorial product $J^{(M)}$ is its gauge covariance, as we discuss now. Under a gauge transform of the type shown in Eq. (2.3) (i.e., a rephasing of the adiabatic wave functions) the exact ADT transforms as[31]

$$\overline{B(\Gamma)}=e^{-i\theta(\mathbf{R}^f)}B(\Gamma)e^{i\theta(\mathbf{R}^i)}. \tag{4.12}$$

Here θ is a diagonal matrix of the phases of the gauge transform angles θ_j [Eq. (2.3)]. Thus the ADT is affected only according to the rephasing at the *end points* $\mathbf{R}^i$ and $\mathbf{R}^f$ of the path: it is invariant to the rephasing of the adiabatic states occurring in the inner points. This property of the ADT is its gauge covariance. We can show that for any finite M, $J^{(M)}$ is gauge covariant as well:

$$\begin{aligned}&\overline{\langle\alpha+1|\alpha\rangle}=e^{-i\theta^{\alpha+1}}\langle\alpha+1|\alpha\rangle e^{i\theta^{\alpha}},\\ &\overline{\langle\alpha+1|\alpha\rangle\langle\alpha|\alpha-1\rangle}=e^{-i\theta^{\alpha+1}}\langle\alpha+1|\alpha\rangle\langle\alpha|\alpha-1\rangle e^{i\theta^{\alpha-1}},\\ &\vdots\\ &\overline{J^{(M)}}=e^{-i\theta^{M}}J^{(M)}e^{i\theta^{1}}.\end{aligned} \tag{4.13}$$

Thus, $J^{(M)}$ for any M behaves under gauge transformation precisely as the exact ADT. This feature is important since it assures that the calculated approximation using a finite number of points is not sensitive to the choice of electronic function phases. It should be mentioned that actually the invariance to the inner point states (states 2,...,$M-1$) can be extended to invariance to any unitary mixing. Namely, even if these intermediate states are mixed by some unitary matrix [member of the unitary $N\times N$ group $U(N)$], the final result is unchanged. Thus the combinatorial matrix product of Eq. (4.9) is locally $U(N)$ invariant for the intermediate states and thus, just like the ADT, it is covariant with respect to $U(N)$.

In general, the matrix product $J^{(M)}$ is not unitary for any finite M, although in the limit $M\to\infty$ it converges to the

unitary ADT. This deviance from unitarity is indicative of the quality of the points from which it is composed. It is expected that a straightforward generalization of the adaptive algorithm described above for CI verification (in the combinatorial invariant) can be constructed here as well, enabling an efficient determination of the points which are needed for the computation of the ADT.

V. SUMMARY AND DISCUSSION

We have presented techniques for the treatment of various aspects of conical intersections. Our methods are based on the concept of the combinatorial invariant and the covariant. We have shown that efficient and robust algorithms for verification and location of a CI can be devised using this concept and we generalized the concept to the non-Abelian case for constructing the ADT matrix along a path.

While the combinatorial invariant converges to the Berry phase only in the limit of infinitely high density of sampling points. It is manifestly gauge invariant, even in a crude discrete limit. This makes the algorithms based on it robust. The adaptive verification algorithm we presented makes full use of the combinatorial invariant by using its properties to decide where points on the path should be added.

Our non-Abelian generalization, the combinatorial covariant product of matrices can be used to produce a matrix which approximates the exact ADT matrix and has exactly the same gauge transformation laws. This yields a method which is expected to be efficient, since we do not need to compute the NACs. It is also robust against spurious gauge choices of the underlying adiabatic basis.

Future work will be devoted to the incorporation of these techniques into general purpose quantum chemistry computer codes. Perhaps, the only fundamentally new element that needs to be added to existing codes is the calculation of the overlap between electronic eigenstates at different nuclear positions.

The recurrent theme in this work is the construction of approximations that *manifestly preserve the correct gauge transformation laws* of their continuous limit counterparts. This is important if such discrete calculations are to yield meaningful and unique results.[31] Gauge covariance is a basic notion in non-Abelian gauge theory where an analogous concept to the ADT arises, the so-called Wilson line.[38,39] In gauge theory, the matrix field analogous to NACs is the *connection* and then Wilson lines are its path-ordered matrix exponentials in much the same way as the ADT is of the NACs [Eq. (4.9)]. Wilson lines were introduced and gained popularity as conceptual and computational tools in parallel to the development of the ADT theory.[27,40] While the connection of the Born-Oppenheimer framework to gauge theory has been noted before,[22,41–43] it should be stressed that the ADT and Wilson line concepts appeared in completely different contexts and serve different purposes.

The concepts presented here are directly applicable to the case of complex (Hermitian) electronic Hamiltonians. While we demonstrated the methods for the real case (where real eigenfunctions can be used and the phase is then simply the sign), the combinatorial invariant and covariant preserve their noted properties for the complex case as well. This will become useful in cases where spin-orbit interactions are considered. In the complex case, use of gauge-covariant methods is critical because the wave functions can vary their phase continuously, while in the real case they only vary their sign.

ACKNOWLEDGMENT

This research was supported by the German Israel Foundation (GIF).

[1] J. von Neumann and E. P. Wigner, Phys. Z. **30**, 467 (1929).
[2] M. R. Manaa and D. R. Yarkony, J. Am. Chem. Soc. **116**, 11444 (1994).
[3] F. Bernardi, M. Olivucci, and M. A. Robb, J. Photochem. Photobiol., A **105**, 365 (1997).
[4] M. Chachisvilis and A. H. Zewail, J. Phys. Chem. A **103**, 7408 (1999).
[5] M. Ben-Nun and T. J. Martinez, Chem. Phys. **259**, 237 (2000).
[6] Y. Haas and S. Zilberg, J. Photochem. Photobiol., A **144**, 221 (2001).
[7] S. A. Trushin, W. Fuss, and W. E. Schmid, Chem. Phys. **259**, 313 (2000).
[8] A. L. Sobolewski and W. Domcke, J. Phys. Chem. A **103**, 4494 (1999).
[9] S. Mahapatra, L. S. Cederbaum, and H. Koppel, J. Chem. Phys. **111**, 10452 (1999).
[10] C. A. Mead and D. G. Truhlar, J. Chem. Phys. **70**, 2284 (1979).
[11] A. Kuppermann and Y. S. M. Wu, Chem. Phys. Lett. **205**, 577 (1993).
[12] R. Baer, D. M. Charutz, R. Kosloff, and M. Baer, J. Chem. Phys. **105**, 9141 (1996).
[13] C. A. Mead, J. Chem. Phys. **70**, 2276 (1979).
[14] S. Matsika and D. R. Yarkony, *Role of Degenerate States in Chemistry*, edited by M. Baer and G. D. Billing (Wiley, New York, 2002), Vol. 124, p. 557.
[15] D. R. Yarkony, Rev. Mod. Phys. **68**, 985 (1996).
[16] I. N. Ragazos, M. A. Robb, F. Bernardi, and M. Olivucci, Chem. Phys. Lett. **197**, 217 (1992).
[17] M. J. Bearpark, M. A. Robb, and H. B. Schlegel, Chem. Phys. Lett. **223**, 269 (1994).
[18] R. Izzo and M. Klessinger, J. Comput. Chem. **21**, 52 (2000).
[19] D. R. Yarkony, J. Phys. Chem. A **108**, 3200 (2004).
[20] H. C. Longuet-Higgins, U. Opik, M. H. L. Pryce, and R. A. Sack, Proc. R. Soc. London **244**, 1 (1958).
[21] M. Baer, *Adv. Chem Phys: Role of Degenerate States in Chemistry*, edited by M. Baer and G. D. Billing (Wiley, New York, 2002), Vol. 124, p. 39.
[22] M. Baer, A. Vibok, G. J. Halasz, and D. J. Kouri, *Advances in Quantum Chemistry* (Academic, London, 2003), Vol. 44, p. 103.
[23] R. D. King-Smith and D. Vanderbilt, Phys. Rev. B **47**, 1651 (1993).
[24] R. Resta, Rev. Mod. Phys. **66**, 899 (1994).
[25] R. Resta, J. Phys. C **12**, R107 (2000).
[26] S. Pancharatnam, Proc. Indian Acad. Sci., Sect. A **44**, 247 (1956).
[27] M. Baer, Chem. Phys. Lett. **35**, 112 (1975).
[28] T. Pacher, L. S. Cederbaum, and H. Koppel, J. Chem. Phys. **89**, 7367 (1988).
[29] H. Koppel, J. Gronki, and S. Mahapatra, J. Chem. Phys. **115**, 2377 (2001).
[30] R. Abrol and A. Kuppermann, J. Chem. Phys. **116**, 1035 (2002).
[31] R. Baer, J. Chem. Phys. **117**, 7405 (2002).
[32] M. V. Berry, Proc. R. Soc. London **392**, 45 (1984).
[33] M. Baer, A. M. Mebel, and R. Englman, Chem. Phys. Lett. **354**, 243 (2002).
[34] F. T. Smith, Phys. Rev. **179**, 111 (1969).
[35] T. Pacher, L. S. Cederbaum, and H. Koppel, Adv. Chem. Phys. **84**, 293 (1993).
[36] M. Baer, J. Phys. Chem. A **104**, 3181 (2000).
[37] M. Baer, Phys. Rep. **358**, 75 (2002).
[38] K. G. Wilson, Phys. Rev. D **10**, 2445 (1974).
[39] M. E. Peskin and D. V. Schroeder, *An Introduction to Quantum Field Theory* (Perseus Pr, Philadelphia, 1995).
[40] M. Baer, Mol. Phys. **40**, 1011 (1980).
[41] R. Englman and A. Yahalom, *Adv. Chem Phys: Role of Degenerate States in Chemistry*, edited by M. Baer and G. D. Billing (Wiley, New York, 2002), Vol. 124, p. 197.
[42] T. Pacher, C. A. Mead, L. S. Cederbaum, and H. Koppel, J. Chem. Phys. **91**, 7057 (1989).
[43] R. Baer, D. J. Kouri, M. Baer, and D. K. Hoffman, J. Chem. Phys. **119**, 6998 (2003).